MCB
Journals.ASM.org

Mice without MacroH2A Histone Variants

John R. Pehrson, Lakshmi N. Changolkar,* Carl Costanzi,* N. Adrian Leu*

Department of Animal Biology, School of Veterinary Medicine, University of Pennsylvania, Philadelphia, Pennsylvania, USA

MacroH2A core histone variants have a unique structure that includes a C-terminal nonhistone domain. They are highly conserved in vertebrates and are thought to regulate gene expression. However, the nature of genes regulated by macroH2As and their biological significance remain unclear. Here, we examine macroH2A function *in vivo* by knocking out both *macroH2A1* and *macroH2A2* in the mouse. While macroH2As are not required for early development, the absence of macroH2As impairs prenatal and postnatal growth and can significantly reduce reproductive efficiency. The distributions of macroH2A.1- and macroH2A.2-containing nucleosomes show substantial overlap, as do their effects on gene expression. Our studies in fetal and adult liver indicate that macroH2As can exert large positive or negative effects on gene expression, with macroH2A.1 and macroH2A.2 acting synergistically on the expression of some genes and apparently having opposing effects on others. These effects are very specific and in the adult liver preferentially involve genes related to lipid metabolism, including the leptin receptor. MacroH2A-dependent gene regulation changes substantially in postnatal development and can be strongly affected by fasting. We propose that macroH2As produce adaptive changes to gene expression, which in the liver focus on metabolism.

MacroH2A core histone variants have a unique structure in which an N-terminal H2A domain is connected to a C-terminal nonhistone domain (1). The H2A domain can substitute for conventional H2A in the nucleosome, and we estimated that ~1 in 30 nucleosomes contains a macroH2A in adult rat liver (1, 2), an organ with relatively high macroH2A content. Most of the nonhistone region consists of an evolutionarily conserved domain (3) called a macrodomain. Macrodomains are found in a variety of proteins and as stand-alone proteins in many bacteria (3, 4). Some, but not all, macrodomains bind ADP-ribose with high affinity (5, 6).

MacroH2As show a complex distribution in metazoan organisms (7). The basal metazoan species *Trichoplax adhaerens* and the sponge *Amphimedon queenslandica* have a macroH2A gene, as does *Hydra magnipapillata*, clearly indicating its presence in early metazoan evolution. While some other invertebrate genomes contain a macroH2A gene, many complete or nearly complete invertebrate genomes lack macroH2A: e.g., *macroH2A* is present in a sea urchin (*Strongylocentrotus purpuratus*), a tick (*Ixodes scapularis*), and an annelid (*Capitella teleta*) but is absent in sequenced insects, a nematode (*Caenorhabditis elegans*), and a tunicate (*Ciona intestinalis*). Two highly conserved macroH2A genes, *macroH2A1* and *macroH2A2*, are found in mammalian genomes, and clearly homologous genes can be found in birds, reptiles, and fish. To our knowledge, macroH2A genes have not been detected in fungal, protozoan, or plant genomes. These findings indicate that macroH2As first appeared in early metazoan evolution and were lost in some invertebrate lineages but were strongly retained in higher vertebrate species.

In mice, humans, and many other vertebrates, *macroH2A1* transcripts are alternately spliced to produce two macroH2A.1 variants, macroH2A.1.1 and macroH2A.1.2, which differ in an ~30-amino-acid region of the macrodomain (1, 8). *macroH2A2* appears to encode a single protein, macroH2A.2, that has the same size and general structure as the macroH2A.1 variants but is only about 70% identical in primary structure (9, 10). The macrodomain of macroH2A.1.1 binds ADP-ribose (6), although the functional significance of this interaction for macroH2A1.1 nucleosomes is unclear. There is no identified small molecule that binds the macrodomains of macroH2A.1.2 or macroH2A.2. MacroH2As are present in all organs that we have examined, including liver, brain, testis, thymus, kidney, and adrenal gland. However, the macroH2A contents and compositions of different tissues can be significantly different (9, 11). For example, macroH2A.1.1 appears to be present mainly in nonproliferating cells of differentiated tissues (11, 12).

Although it is generally believed that regulation of gene expression is an important role for macroH2As, there is no consensus on the nature of the genes that are targeted or the biological significance of this regulation. A study of gene expression in MACROH2A1 knockdown MCF-7 cells indicated that macroH2A.1 impacts the expression of many genes, with 19% of 97 genes examined showing significantly altered expression (13). A role in gene silencing is suggested by the preferential localization of macroH2As to domains of transcriptionally silent heterochromatin, including the inactive X chromosome (9, 10, 14), pericentromeric heterochromatin in some cells (15, 16), the XY body of spermatocytes (17), and transcriptionally silent senescence-associated heterochromatic foci (18). Cell-type-specific macroH2A-dependent silencing of interleukin-8 (IL-8) was observed in studies of cultured cell lines (19), suggesting that macroH2As could be important for establishing or maintaining cell-type-specific patterns of gene expression. Other studies indicate that macroH2As have a critical role in early development and

Received 16 June 2014 **Returned for modification** 15 July 2014
Accepted 2 October 2014

Published ahead of print 13 October 2014

Address correspondence to John R. Pehrson, pehrson@vet.upenn.edu.

* Present address: Lakshmi N. Changolkar, Department of Pathology and Lab Medicine, University of Pennsylvania, Philadelphia, Pennsylvania, USA; Carl Costanzi, Western Maine Health, Norway, Maine, USA; N. Adrian Leu, Department of Human Genetics, The University of Utah, Salt Lake City, Utah, USA.

Supplemental material for this article may be found at http://dx.doi.org/10.1128/MCB.00794-14.

doi:10.1128/MCB.00794-14

differentiation. A knockdown of *macroH2A2* in developing zebrafish embryos led to severe developmental defects (20), and some studies of embryonic stem (ES) cells found that knockdown of *macroH2A1* and/or *macroH2A2* impaired the expression of differentiation genes and the inactivation of pluripotency genes during *in vitro* differentiation (21, 22). In contrast, our studies of *macroH2A1* knockout (KO) mice showed no obvious defects in development or X inactivation (23). Changes in liver gene expression were seen for a few genes that functionally cluster in the area of metabolism. Most of these genes showed macroH2A.1 enrichment (24), suggesting that they are direct targets of macroH2A.1 nucleosomes. Our results seemed to be inconsistent with the studies that showed dramatic effects on early development and stem cell differentiation. One potential contributor to this apparent inconsistency is macroH2A.2, which could have overlapping functions with macroH2A.1 variants and mask significant aspects of macroH2A function in *macroH2A1* KO mice. To address this possibility and expand our understanding of macroH2A function *in vivo*, we knocked out *macroH2A2* and generated mice that lack both macroH2A.1 and macroH2A.2 histone variants.

MATERIALS AND METHODS

Mice. The University of Pennsylvania Institutional Animal Care and Use Committee approved all animal protocols. Mice were maintained on a 12-h day/night cycle with the lights coming on at 8 a.m. Mice used for organ harvest were euthanized with CO_2 between 9 and 11 a.m. For dual energy X-ray absorptiometry (DEXA) body composition analyses, the mice were anesthetized (100 mg ketamine/kg of body weight plus 10 mg xylazine/kg) and scanned (PIXImus; GE Lunar). MacroH2A KO mice are available through the Mutant Mouse Regional Resource Center (MMRRC) at JAX under the following numbers: C57BL/6 *macroH2A1* KO, 37472; C57BL/6 *macroH2A2* KO, 37474; 129/S6 *macroH2A1 macroH2A2* double KO, 37356.

MacroH2A KO mice. *macroH2A1* KO mice inbred in either the C57BL/6 or 129/S6 (Taconic) background for at least 10 generations were produced as previously described (23). Genotyping was done with a small piece of the tail that was digested with proteinase K. Primers were F1, TCTTTGCAAGGGTCAGACG; R1, ACTGGAGACAGCGCATTACC; and R2, CAACATAACCACCATGATCTCG. Reactions used *Taq* polymerase (New England BioLabs) and an annealing temperature of 55°C (normal allele, 148 bp; KO allele, 238 bp).

The *macroH2A2* (*H2afy2*) KO targeting vector was based on an ~6.8-kb BglII-KpnI fragment of mouse genomic DNA cloned into the pPNT vector (25) (see Fig. S1 in the supplemental material). The Neo cassette was flanked by LoxP recombination sites and inserted into an EaeI site located less than 300 bp upstream of exon 2. A third LoxP site was inserted into an EaeI site located less than 150 bp downstream of exon 2. The targeting vector was electroporated into V6.5 ES cells (26). ES cells positive for homologous recombination by Southern blotting (see Fig. S1) were injected into blastocysts, and the chimeric males were mated to obtain germ line transmission. Recombinant mice were bred with an EIIa Cre mouse (Jackson Laboratories), and offspring were screened by PCR to identify mice carrying KO alleles. The *macroH2A2* KO allele was backcrossed into the C57BL/6 and 129/S6 backgrounds for 10 or more generations. Genotyping primers were AF1, CCCAGCCAATCCCAAGTATG AGG, and CR1, CCCCAACTCACTCCATATGCAGC. Tail DNA PCRs used AccuPrime *Taq* polymerase (Invitrogen) and an annealing temperature of 55°C (normal allele, 895 bp; KO allele, 320 bp) (see Fig. S1).

Microarrays. Wild-type and macroH2A KO females were superovulated and mated with wild-type or macroH2A KO males, respectively. Wild-type and KO embryos were collected, mixed together, and transferred to wild-type pseudopregnant females. Livers were collected from 18.5-day-postcoitum (dpc) fetuses. In studies involving adult mice, wild-type and KO mice were raised together following weaning and were euthanized at 2 months of age at ~10 a.m. The liver was immediately dissected and frozen in liquid nitrogen. Total RNA was isolated using TRIzol (Invitrogen).

Labeled cDNA was prepared from 250 ng of total RNA using the Ambion WT Expression kit (Life Technologies). Labeled cDNA (5.5 μg) was hybridized to mouse gene 2.0 ST GeneChips (adult livers) or mouse gene 1.0 ST GeneChips (fetal livers) (Affymetrix Inc., Santa Clara, CA). The microarrays were stained with streptavidin-phycoerythrin. A GeneChip 3000 7G scanner was used to collect the fluorescence signal.

Affymetrix Command Console and Expression Console were used to quantitate expression levels for targeted genes; default values provided by Affymetrix were applied. Border pixels were removed, and the average intensity of pixels within the 75th percentile was computed for each probe. The average of the lowest 2% of probe intensities occurring in each microarray sector was subtracted as background from all features in that sector. Affymetrix cel files (containing probe intensities) were imported into Partek Genomics Suite (v6.6; Partek, Inc., St. Louis, MO) where robust multiarray average normalization was applied, yielding $\log_2$-transformed intensities for all transcript identifiers (IDs). Normalized intensities were exported from Partek into R, where significance analysis of microarrays (SAM; using the samr v2.0 package [27]) was applied, yielding a fold change and *q* value (false discovery rate [FDR]) for each transcript ID.

Real-time PCR. Total RNA was prepared from mouse liver using TRIzol (Invitrogen). We synthesized cDNA using random hexamer primers and Moloney murine leukemia virus (M-MuLV) reverse transcriptase (RNase H^-) (New England BioLabs) under standard conditions. Real-time PCR was performed, and data were quantitated using the LightCycler System (Roche Applied Science) as previously described (28). Primer sequences and annealing temperatures are listed in Table S5 in the supplemental material.

Purification of macroH2A nucleosomes. MacroH2A-containing mono- and oligonucleosomes were purified from bulk chromatin by thioaffinity chromatography as described previously (28). Briefly, 50 mixed-gender 18.5-dpc fetal mouse livers were very gently homogenized using a Potter-Elvehjem tissue homogenizer, and nuclei were purified by ultracentrifugation through a sucrose cushion; fetal liver nuclei must be handled with care to avoid aggregation. An H1-stripped chromatin fraction was prepared and digested to mono- and oligonucleosomes. H1 removal was done at 60 mM NaCl instead of the 50 mM concentration previously used, which improved removal. Nuclease digestions used recombinant micrococcal nuclease (New England BioLabs), and the protease inhibitor cocktail cOmplete (Roche) was used throughout the procedure. The solubilized nucleosomes were first passed through a column of activated thiol Sepharose (GE Healthcare Life Sciences), which was connected in tandem to a column of thiopropyl Sepharose (GE Healthcare Life Sciences). The columns were disconnected and washed and eluted as previously described (28), except that we first washed the activated thiol Sepharose column with 0.5 M NaCl, 1 mM EDTA, 10 mM Tris (pH 7.5) prior to elution with 100 mM β-mercaptoethanol, 100 mM NaCl, 1 mM EDTA, 10 mM Tris (pH 7.5). This elution procedure was also used for the thiopropyl Sepharose column; the 0.5 M NaCl wash removes nucleosomes bound to the column through cysteine-containing nonhistone proteins. The same thioaffinity procedure was used for a control experiment done with ~50 double KO 18.5-dpc livers.

High-throughput sequencing and mapping of sequences. Mononucleosomal DNA was purified from an agarose gel, and the DNA ends were repaired using standard procedures. An A was added to the 3′ ends using Klenow fragment (3′→5′ exo-), and Illumina multiplex adaptors were ligated to the fragments according to standard procedures. Ligated fragments were gel purified and amplified using Illumina multiplex primers. Libraries were sequenced to 50 bp using an Illumina HiSeq 2000 sequencer. Reads were aligned to the mouse genome (release mm9) using Bowtie, allowing up to 3 mismatches using the flags -v 3 -k 1 -m 1 –best

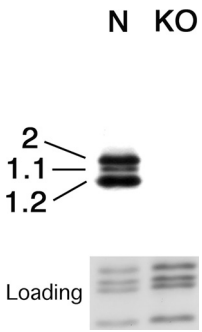

FIG 1 Absence of macroH2A.1 and macroH2A.2 in *macroH2A* double KO mice. Kidney extracts were analyzed on a Western blot that was probed with a mixture of antibodies against macroH2A.1.1, -.1.2, and -.2. Lanes: N, normal mouse kidney; KO, *macroH2A* double knockout kidney. Coomassie blue-stained core histones are shown as a loading control.

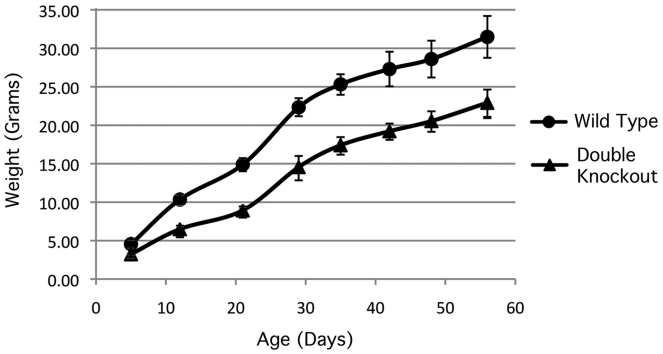

FIG 2 *macroH2A* double KO mice are smaller. Average weights of C57BL/6 double KO ($n = 5$) and wild-type ($n = 8$) mice are shown. Two-tailed t test, $P \leq 0.0004$ at all ages.

–strata. The sequences were deposited in the NCBI GEO database (see below). For the comparison of the macroH2A.1 track (thiopropyl eluted) to the macroH2A.2 track (activated thiol eluted) (see Fig. 4C), the macroH2A-over-input (starting material) ratios were computed by tabulating the expected center of fragments corresponding to each read and then assigning them to sliding-window bins. The $\log_2$ ratio was computed with a pseudocount of 1 added to both macroH2A and input read totals. Bins that had 0 macroH2A and input reads were discarded. The $\log_2$ ratios were normalized by subtracting the genome-wide median $\log_2$ ratio.

Western blots. Proteins were separated by SDS-gel electrophoresis, transferred to polyvinylidene difluoride membranes (11), and probed with rabbit polyclonal antibodies raised against the nonhistone regions of rat macroH2A1.1 and -1.2 and human macroH2A.2 (14). The signal was detected by chemiluminescence. The blot in Fig. 1 used a low-bisacrylamide SDS-polyacrylamide gel, which allows the resolution of all three macroH2A variants (9). The blots in Fig. 3 and 4 and in Fig. S2 in the supplemental material used a gel with a standard acrylamide/bisacrylamide ratio of 37.5:1, which does not resolve macroH2A.1.1 from macroH2A.1.2.

Nucleotide sequence accession number. The normalized data and cel files for the microarray experiments and the high-throughput reads for macroH2A and control nucleosomal DNAs were deposited in the NCBI GEO database under accession number GSE57089.

RESULTS

Knockout of *macroH2A2*. We knocked out *macroH2A2* by removing the second exon (see Materials and Methods and Fig. S1 in the supplemental material). This exon contains the initiator methionine and encodes the first 57 amino acids of the histone region of macroH2A.2. As in the case of the knockout of *macroH2A1*, the *macroH2A2* KO did not produce any obvious developmental defects or reproductive problems. We kept a small group of *macroH2A2* KO and wild-type mice in a mixed C57BL/6 × 129/Sv background for more than 1.5 years and did not observe any obvious pathology in the KOs in comparison to controls.

The *macroH2A2* KO allele was backcrossed into the C57BL/6 and 129/S6 (Taconic) backgrounds for 10 or more generations, which should eliminate most background effects except for regions closely linked to *macroH2A2* (*H2afy2*). We used an F1 (C57BL/6 × 129/Sv) ES cell line, and sequence polymorphisms around *macroH2A2* showed that the KO allele is from the 129/Sv background. Our *macroH2A1* KO allele is also in the 129/Sv background. The phenotypic effects of the *macroH2A* double KO are different in the C57BL/6 and 129/S6 backgrounds as described below.

Normal development in the absence of macroH2A. We were able to produce *macroH2A* double KO males and females, and Western blotting confirmed the absence of macroH2A.1 and macroH2A.2 (Fig. 1). External and internal examination of late-stage fetuses, newborn pups, and adults did not reveal any obvious structural defects associated with the absence of macroH2As. We did a histological examination of major organs and tissues from two young adult double KOs and an age-matched control and did not observe any obvious anomalies or pathology in the double KOs. These results show that mouse development can proceed in an apparently normal fashion in the absence of macroH2A variants.

Reproductive problems of C57BL/6 *macroH2A* double KOs. We efficiently bred *macroH2A* double KOs with one another in the 129/S6 background, but C57BL/6 double KOs bred very poorly with one another. In some cases, the female did not appear to become pregnant, while in other cases many or all of the pups died or were eaten shortly after birth. Young adult C57BL/6 double KOs typically produced offspring when bred with wild-type mice or mice expressing at least one *macroH2A* gene, showing that these mice are not generally infertile. We believe that the effects of the *macroH2A* double KO exacerbate reproductive and mothering problems that occur with wild-type C57BL/6 mice (29). In addition, double KOs appear to be more susceptible to perinatal death (see below).

Reduced size of *macroH2A* double KOs. Double KO pups in both the 129/S6 and C57BL/6 backgrounds were smaller on average than wild-type pups, and this difference persisted into adulthood. To demonstrate these effects, we mixed wild-type and double KO preimplantation embryos and implanted them into wild-type recipient females. An experiment tracking the weights of double KO and wild-type C57BL/6 males is shown in Fig. 2, and similar results were observed with females. We used dual-energy X-ray absorptiometry (DEXA) to analyze the size and body composition of 129/S6 adult double KO and control males (Table 1). The double KOs weighed less and were 9% shorter in length. Most of the weight difference was accounted for by reduced lean body mass. The bone mineral content, bone mineral density, and fat content of the double KOs were not significantly different from those of their wild-type littermates.

We used C57BL/6 mice to examine whether the absence of macroH2As reduced the size of late-stage fetuses. We bred double KO males with females that were heterozygous for *macroH2A1*

TABLE 1 Body composition analysis of *macroH2A* double KO adults[a]

Parameter	Result by genotype: Wild type ($n = 5$)	Double KO ($n = 5$)	P value[b]
Wt (g)	27.9 ± 1.9	23.2 ± 1.8	0.0035
Length (cm)	10.1 ± 0.3	9.2 ± 0.2	0.0017
BMD (g/cm^2)	0.07 ± 0.008	0.07 ± 0.007	0.91
BMC (g)	0.56 ± 0.07	0.52 ± 0.05	0.41
Lean (g)	20.6 ± 1.2	16.6 ± 1	0.001
Fat (g)	8.0 ± 1.4	7.1 ± 1.4	0.42
% fat	27.8 ± 3	29.6 ± 3.9	0.47

[a] Body composition was measured by DEXA. Mice were 15-week-old males in the 129/S6 background. BMD, bone mineral density; BMC, bone mineral content.
[b] One-tailed *t* test.

and KO for *macroH2A2*. Fetuses were collected at 17.5 and 18.5 days postcoitum (dpc). We obtained an equal number of double KO fetuses and fetuses that were heterozygous for *macroH2A1* and KO for *macroH2A2*, but the double KO fetuses were smaller (Table 2). A similar result was obtained with a group of fetuses that were produced by breeding double KO males with females that were KO for *macroH2A1* and heterozygous for *macroH2A2* (Table 2).

The reduced size of late-stage double KO fetuses and the slower growth of double KO pups and young adults show that the absence of macroH2As impairs pre- and postnatal growth. This suggests a role for macroH2As in regulating metabolic, neurologic, and/or hormonal controls of growth. Our previous discovery that macroH2A.1 variants regulate metabolic genes in the liver is consistent with this idea, although the absence of macroH2A.1 by itself did not have any obvious effect on growth.

Increased perinatal death of C57BL/6 *macroH2A* double KOs. Our breeding experiences found a deficiency in the number of C57BL/6 double KOs that survived to the age of weaning (3 weeks). Table 3 summarizes the results that we obtained when we bred mice with different combinations of *macroH2A* KO alleles. Overall, the number of *macroH2A* double KOs produced was ~29% less than expected based on the genotypes of the parents. We observed significant numbers of mice dying shortly after birth, and genotype analyses of 25 dead newborns found a strong bias toward double KOs (84%). Interestingly, we did not observe a significant deficiency of double KOs in our studies of 71 late-stage fetuses (Table 2). Taken together, these results indicate that the perinatal period is the important time when *macroH2A* double KOs were lost. More double KO females survived to weaning than males, although the difference was small; this indicates that issues related to X inactivation are unlikely to be a major factor in the loss of double KO females.

Additional phenotypic effects in 129/S6 *macroH2A* double KO mice. Double KO 129/S6 mice frequently showed signs of bilaterally increased palpebral fissure in comparison to controls. Histological analysis of the globes did not reveal any abnormalities, and histological analysis of the heads found no orbital mass or cyst that could cause a protrusion of the globes. We conclude that this is a true macroblepharon due to an abnormally increased length of the eyelid margin. Some double KOs developed eyelid inflammation—typically between 6 and 12 months of age—possibly secondary to eye irritation caused by the wider eyelid margin.

Some 129/S6 *macroH2A* double KO mice showed increased darkening of the hair on their back. This effect appeared at ~6 weeks of age and was typically more evident in young adults than in older mice.

MacroH2A-dependent gene regulation in development—fetal liver. Our current hypothesis is that gene regulation is an important function of macroH2A histones. Our previous studies of *macroH2A1* KO mice identified genes that appear to be regulated by macroH2A.1 in adult liver but not in neonatal liver (23). To increase our understanding of the developmental aspect of macroH2A function, we used microarrays to examine gene expression in 129/S6 double KO fetal liver (18.5 dpc); six double KOs were compared to six controls, with the control livers coming from wild-type fetuses that developed together with the double KOs in wild-type recipient females. The macroH2A.1 content of late fetal liver is lower than that of adult liver and consists almost entirely of macroH2A.1.2 (11, 23). The macroH2A.2 content of late fetal liver is relatively low but is higher than that in adult liver (Fig. 3).

Remarkably few genes showed altered expression in our microarray analysis of double KO fetal liver. Twenty genes showed a 1.5-fold or more increase in expression in the double KOs, but only *Npy* (encoding neuropeptide Y) and *Serpina7* (encoding thyroxine binding globulin) showed a low false discovery rate. *Pip5k1b* (encoding a phosphatidylinositol-4-phosphate kinase) showed a 2-fold decrease in expression with a low false discovery rate, but no other genes showed more than a 2-fold decrease in expression. The increased expression of *Npy* and *Serpina7* and the decreased expression of *Pip5k1b* were confirmed by a real-time PCR analysis of a larger group of fetal livers (Table 4). We also used real-time PCR to examine the expression of some genes that showed a smaller change in expression and a false discovery rate of <10% and confirmed a few additional genes with smaller but significant changes in expression (Table 4). See Table S1 in the supplemental material for a list of all microarray genes with a false discovery rate of <10%.

We used *macroH2A1* and *macroH2A2* single KO fetuses to assess the contributions of macroH2A.1 and -.2 variants to the regulation of *Npy*, *Serpina7*, and *Pip5k1b* (Table 4). Surprisingly, *macroH2A1* KO fetal liver showed decreased *Npy* expression, while *macroH2A2* KO fetal liver showed increased expression.

TABLE 2 Smaller size of *macroH2A* double KO fetuses[a]

Fetal age (dpc)	Avg wt (g) for genotype: *macroH2A1*$^{+/-}$ *macroH2A2*$^{-/-}$	*macroH2A1*$^{-/-}$ *macroH2A2*$^{+/-}$	*macroH2A1*$^{-/-}$ *macroH2A2*$^{-/-}$	P value[b]
17.5	0.80 ± 0.02 ($n = 4$)		0.70 ± 0.03 ($n = 4$)	0.004
18.5	1.15 ± 0.08 ($n = 24$)		1.07 + 0.1 ($n = 24$)	0.003
18.5		1.09 ± 0.08 ($n = 9$)	1.01 ± 0.08 ($n = 6$)	0.04

[a] Mice were in the C57BL/6 background. Parental genotypes: males were double KO, and females were KO for one macroH2A gene and heterozygous for the other.
[b] One-tailed *t* test.

TABLE 3 Decreased survival of C57BL/6 *macroH2A* double KO mice

Parental genotype	No. of pups weaned	Double KO			
		No. weaned	% of total	Expected % of total[a]	P^b
macroH2A1$^{+/-}$ *macroH2A2*$^{+/-}$ × *macroH2A1*$^{+/-}$ *macroH2A2*$^{+/-}$	75	2	2.7	6.25	0.14
macroH2A1$^{+/-}$ *macroH2A2*$^{-/-}$ × *macroH2A1*$^{-/-}$ *macroH2A2*$^{+/-}$	75	15	20	25	0.19
macroH2A1$^{-/-}$ *macroH2A2*$^{+/-}$ × *macroH2A1*$^{+/-}$ *macroH2A2*$^{-/-}$	27	5	19	25	0.3
macroH2A1$^{+/-}$ *macroH2A2*$^{-/-}$ × *macroH2A1*$^{-/-}$ *macroH2A2*$^{-/-}$	228	89	39	50	0.00056
macroH2A1$^{-/-}$ *macroH2A2*$^{+/-}$ × *macroH2A1*$^{-/-}$ *macroH2A2*$^{-/-}$	50	9	18	50	2.8×10^{-6}
Total	455	120	26	37	6.4×10^{-7}

[a] Based on parental genotypes.
[b] Cumulative binomial probability.

This indicates that macroH2As can exert positive and negative regulatory effects on the same gene. The expression of *Serpina7* and *Pip5k1b* was unchanged in *macroH2A1* and *macroH2A2* single knockout fetal liver, indicating that macroH2A.1 and macroH2A.2 have a synergistic effect on these genes.

To investigate how macroH2A function changes during postnatal development, we compared the gene expression effects of a *macroH2A* double KO in fetal liver to those seen in adult liver. We previously found that *ATP11a*, *Krt23*, *Lpl*, *Serpina7*, and *Vldlr* showed increased expression in *macroH2A1* KO adult liver (23), and real-time PCR analysis of these genes in double KO adult liver showed similar or larger increases in expression (Table 5, DKO nonfasting). Interestingly, *ATP11a*, *Krt23*, *Lpl*, and *Vldlr* showed essentially no change in our microarray analysis of fetal liver, and real-time PCR confirmed that the expression of *Krt23* and *Lpl* was unchanged in double KO fetal liver (Table 4, DKO fetal). We also examined the expression of *Npy* and *Pip5k1b* in adult liver. While *Pip5k1b* showed decreased expression in both adult and fetal double KO liver, *Npy* expression in adult liver was unaffected by the absence of macroH2A (Table 4, DKO adult). These results demonstrate that macroH2A-dependent regulation of gene expression changes substantially in going from late fetal liver to adult liver.

Assessing the potential functions of macroH2As in fetal liver is difficult since few genes appear to be affected. We previously identified *Serpina7* as a macroH2A.1 target gene in adult liver (23), and its involvement in thyroxine transport is consistent with a role for macroH2As in metabolic regulation. In the central nervous system, neuropeptide Y has important functions related to energy homeostasis. Its functions in the liver are less clear, but there is evidence that it can regulate hepatic glucose metabolism (30). Pip5k1β generates phosphatidylinositol-4,5-bisphosphate, which is a key substrate in signaling pathways that regulate many cellular functions (31), including potentially hepatic glucose metabolism (32).

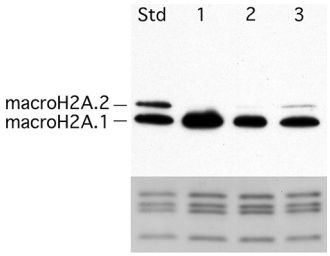

FIG 3 MacroH2A composition of mouse liver. Western blotting of total nuclear extracts using a mixture of macroH2A.1 and macroH2A.2 antibodies. Std, extract of adult mouse kidney; lane 1, adult mouse liver; lane 2, 3-day mouse liver; lane 3, 18.5-day fetal mouse liver. Coomassie blue-stained core histones are shown as a loading control. The positions of macroH2A.1 and macroH2A.2 were determined using extracts from *macroH2A1* and *macroH2A2* single KOs (see Fig. S2 in the supplemental material). MacroH2A.1.1 and -1.2 ran as a single band on this gel.

MacroH2A-dependent gene regulation in adult liver—effects of fasting. We used microarrays to examine the effects of a *macroH2A* double KO on gene expression in the livers of 2-month-old 129/S6 adult males. The mice in this study (5 wild type and 5 double KOs) were fasted overnight before liver collection. We did this in an attempt to reduce variation in gene expression related to metabolic status and to examine whether the effects of macroH2As on gene expression are influenced by metabolic status. This analysis identified 20 genes/transcripts that were increased by more than 2-fold with a false discovery rate of <10% and 7 genes/transcripts that had decreased expression of more than 2-fold with a false discovery rate of <10%. We examined the expression of 10 of these genes by real-time PCR, focusing on genes that had some functional characterization and that had not already been identified by our analysis of *macroH2A1* KO liver. Eight of these genes showed statistically significant changes in expression (*t* test, $P < 0.05$) by real-time PCR (Table 5, DKO fasting), while the other 2, *Arfip1* and *Selenbp2*, showed no significant change (see Tables S2 and S3 in the supplemental material for a list of all microarray genes/transcripts that showed >1.5-fold change in expression and a false discovery rate of <10%).

Three of these genes are notable for large changes in expression: *Cml5* (4.1-fold increase) encodes a poorly characterized protein that appears to be an *N*-acetyltransferase (33), *Fabp5* (3.5-fold increase) encodes a cytosolic fatty acid binding protein that can influence glucose and lipid metabolism (34), and *Lcn13* (16-fold decrease) encodes a secreted lipid binding protein that can regulate glucose and lipid metabolism (35, 36). These results reinforce our previous finding that macroH2A.1 has a role in regulating metabolism-related genes, especially genes related to lipid metabolism (23, 24). Two of the other 5 new genes also have a clear connection to lipid metabolism: *Lepr* (1.9-fold increase) encodes the receptor for leptin, an adipokine that has a central role in energy homeostasis (37), and *Rgs16* (2.3-fold increase) encodes a GTPase-activating protein that can regulate fatty acid and glucose metabolism in the liver (38). The proteins encoded by the other 3 genes do not have any obvious connection to lipid metabolism:

TABLE 4 Relative gene expression in *macroH2A* KO liver[a]

	Result for group:							
	DKO fetal[b]		*macroH2A1*$^{-/-}$ fetal[c]		*macroH2A2*$^{-/-}$ fetal[d]		DKO adult[e]	
Gene	Expression[f]	*P* (*t* test)[g]	Expression	*P* (*t* test)	Expression	*P* (*t* test)	Expression	*P* (*t* test)
Npy	3.9	0.0009	0.25	0.006*	1.7	0.004*	1.1	0.27
Serpina7	2.3	2×10^{-6}	0.8	0.37*	0.89	0.56*	5.0	0.0009
Pip5k1b	0.5	3×10^{-7}	0.92	0.62	0.95	0.47	0.66	0.04
Pou2af1	0.69	0.0024						
Herc5	0.78	4×10^{-6}						
Ebf	0.78	0.004						
Spi-B	0.77	0.02						
Krt23	0.87	0.58*					6.0	4×10^{-8}
Lpl	1.1	0.53					3.0	1×10^{-7}

[a] Livers were from 18.5-dpc fetuses or 2-month-old adult males, 129/S6 background.
[b] Fourteen double KO and 11 control livers were analyzed.
[c] Nine *macroH2A1* KO and 11 control livers were analyzed.
[d] Twelve *macroH2A2* KO and 11 control livers were analyzed.
[e] Eleven double knockout and 13 control livers were analyzed.
[f] Relative expression, double KO/normal, was determined by real-time PCR.
[g] *t* test *P* values are one-tailed except as indicated by asterisks, where they are two-tailed.

Sdf2l1 (2.6-fold increase) appears to be a subunit of an endoplasmic reticulum chaperone complex, Vtcn1 (2.5-fold increase) is a T-cell activation inhibitor, and Hamp2 (2.4-fold decrease) is thought to be an antimicrobial peptide that also regulates iron uptake.

To examine whether fasting was a factor in the macroH2A-dependent regulation of these genes, we examined the expression of 6 of them in nonfasting adult livers (Table 5, DKO nonfasting). The results with *Lepr* and *Lcn13* were similar in fasting and nonfasting double KO liver. In contrast, *Fabp5*, *Rgs16*, and *Sdf2l1* did not show statistically significant changes in nonfasting double KO liver. Interestingly, *Cml5* expression, which showed a 4-fold increase in double KO fasting liver, showed a 3.3-fold decrease in nonfasting double KO liver. These results show that nutritional status can have a strong effect on macroH2A-dependent gene regulation.

We investigated the individual contributions of *macroH2A1* and *macroH2A2* to the regulation of *Lcn13*, *Serpina7*, and *Cml5* in nonfasting adult liver (Table 5). Our results indicate that both *macroH2A1* and *macroH2A2* contribute to the activation of *Lcn13*, with *macroH2A1* having the bigger effect. It is not clear whether *macroH2A2* contributes to the repression of *Serpina7* in adult liver since the effect of a *macroH2A2* KO was small and of low significance. *Cml5* expression was lower in *macroH2A1* KO liver but interestingly was higher in *macroH2A2* KO liver. This resembles the situation that we found for *Npy* in fetal liver, with *macroH2A1* and *macroH2A2* single KOs having opposite effects on the same gene.

TABLE 5 Relative gene expression in *macroH2A* KO adult liver[a]

	DKO fasting[b]		DKO nonfasting[c]		*macroH2A1*$^{-/-}$ nonfasting[d]		*macroH2A2*$^{-/-}$ nonfasting[e]	
Gene	Expression[f]	*P* (*t* test)[g]	Expression	*P* (*t* test)	Expression	*P* (*t* test)	Expression	*P* (*t* test)
Cml5	4.1	0.001	0.3	0.04*	0.42	0.01*	2.6	0.04*
Fabp5	3.5	4.5×10^{-5}	1.3	0.15				
Sdf2l1	2.6	3.1×10^{-5}	0.95	0.77*				
Vtcn1	2.5	0.008						
Rgs16	2.3	0.007	1.4	0.26				
Lepr	1.9	0.005	1.4	0.01				
Hamp2	0.42	0.04						
Lcn13	0.06	9×10^{-6}	0.06	0.0001	0.12	2.4×10^{-6}	0.33	0.02
Serpina7			5.0	0.0009	3.7	2.3×10^{-5}	1.3	0.15
ATP11a			2.8	1.1×10^{-7}				
Lpl			3.0	1.2×10^{-7}				
Krt23			6.0	3.9×10^{-8}				
Vldlr			1.7	0.0008				

[a] Livers were from 2-month-old males, 129/S6 background. DKO, double KO.
[b] Eight double KO and 8 control livers were analyzed.
[c] Eleven double KO and 13 control livers were analyzed.
[d] Nine *macroH2A1* KO and 9 control livers were analyzed.
[e] Eight *macroH2A2* KO and 8 control livers were analyzed.
[f] Relative expression, double KO/normal, was determined by real-time PCR.
[g] *t* test *P* values are one-tailed except as indicated by asterisks, where they are two-tailed.

MacroH2A.1 and macroH2A.2 nucleosomes have overlapping distributions. Our gene expression studies indicate that macroH2A.1 and macroH2A.2 nucleosomes can regulate the same genes, which suggested that there might be overlap in their distributions in chromatin. We examined this possibility with fetal liver, because the macroH2A.2 content of fetal liver is higher than that of adult liver (Fig. 3). Previously, we used thioaffinity chromatography to purify macroH2A.1 nucleosomes from adult mouse liver using a two-stage thioaffinity chromatography method (28). We used this approach because it is highly effective and our attempts to immunoprecipitate macroH2A nucleosomes proved unsatisfactory. In this method, nuclease-digested chromatin is first passed through activated thiol Sepharose, which does not bind macroH2A.1 nucleosomes but does bind many cysteine-containing proteins. The chromatin is then passed through thiopropyl Sepharose, which binds macroH2A.1 nucleosomes. A salt wash is used to remove nucleosomes bound by cysteine-containing nonhistone proteins, and the macroH2A.1 nucleosomes are then eluted with mercaptoethanol. As expected, the macroH2A.1 nucleosomes from fetal liver were bound to thiopropyl Sepharose (Fig. 4A, Western blot). Surprisingly, the macroH2A.2 nucleosomes were bound to the activated thiol Sepharose column. The spacer arms of these thioaffinity matrices are different, and there is an additional cysteine in the macrodomain of macroH2A.2 that may account for this difference.

To assess the purity of the thiopropyl and activated thiol macroH2A nucleosomes, we did an experiment with an equivalent number of *macroH2A* double KO fetal livers. No histones or nucleosomal DNA were detected in the thiopropyl-eluted fraction with double KO fetal liver (Fig. 4A, Double Knockout Liver). Based on the intensity of the core histone and nucleosomal DNA bands seen for these fractions with normal liver, we feel that we would have easily detected 10% contamination of this fraction by nonmacroH2A-containing chromatin fragments. As we have previously discussed (24, 28), the presence of conventional H2A in these fractions reflects the interspersion of macroH2A-containing nucleosomes with nucleosomes that contain conventional H2As. In addition, *in vitro* reconstitution experiments indicate that macroH2A.1 preferentially pairs with conventional H2A in the nucleosome core (39). The double KO activated thiol-eluted fractions had a low level of core histones and nucleosomal DNA. Although it is difficult to give a specific estimate of the level of non-macroH2A.2-containing chromatin fragments in this fraction from normal liver, a side-by-side comparison of the activated thiol-eluted fractions from wild-type and double KO liver (see Fig. S4 in the supplemental material) clearly indicates that more than 50% of the chromatin fragments in the activated thiol-eluted fractions from the normal fetal liver contain macroH2A.2. The effective separation of macroH2A.1 from macroH2A.2 by our procedure clearly indicates that macroH2A.1 and macroH2A.2 rarely occupy the same nucleosome, at least in fetal mouse liver.

The absence of detectable macroH2A in the flowthrough fraction (Fig. 4A, lane FT, Western blot) indicates that we have captured most of the macroH2A nucleosomes on our columns. Using scans of the Western blots from this experiment, we estimated that we recovered ~34% of the macroH2A.1 and ~23% of the macroH2A.2 in the eluted fractions shown in Fig. 4 (see Table S4 in the supplemental material for these calculations). As with any chromatin purification method, it is possible that we lost specific subpopulations of macroH2A nucleosomes during our procedure.

We produced genome-wide macroH2A maps by sequencing mononucleosomal DNA from the thiopropyl-eluted fraction (macroH2A.1 nucleosomes) and the activated thiol-eluted fraction (primarily macroH2A.2 nucleosomes). We also sequenced mononucleosomal DNA from the starting material nucleosomes and the *macroH2A* double KO activated thiol-eluted fraction. A 3-Mbp segment of chromosome 19 illustrates many of the features of these maps (Fig. 4B). As expected, the starting material map shows a relatively even distribution of sequences across the genome, with occasional blank spots and small spikes often caused by repetitive sequences. A similar pattern is seen with the double KO activated thiol map, indicating that these nucleosomes, which contaminate our macroH2A.2 nucleosome fraction, are relatively evenly distributed across the genome. Our previous study of macroH2A.1 distribution in adult liver found that macroH2A.1 is typically organized in relatively large domains that can be enriched, neutral, or depleted for macroH2A.1 nucleosomes. The transcribed regions of most active genes were strongly depleted of macroH2A.1, while inactive genes showed no strong bias toward depletion or enrichment (24). Our new fetal liver macroH2A.1 map appears consistent with these findings, showing domains of enrichment, neutral domains, and discrete domains of depletion that correspond to genes (Fig. 4B).

The fetal liver macroH2A.2 map is remarkably similar to the macroH2A.1 map, showing essentially overlapping domains of enrichment and depletion (Fig. 4B). We examined this on a genome-wide basis by calculating the macroH2A.1 content (thiopropyl eluted relative to starting material) and macroH2A.2 content (activated thiol eluted relative to starting material) in sliding windows across the genome. A plot of these data (Fig. 4C) shows a strong correlation between macroH2A.1 and macroH2A.2 content. In general, the height of peaks of enrichment and the depth of depletion seen over genes are less for the macroH2A.2 map (Fig. 4B and C), which we believe is at least partly due to the presence of non-macroH2A nucleosomes in this fraction. The overlapping distributions of macroH2A.1 and macroH2A.2 nucleosomes provide a straightforward explanation for how genes can be regulated by both macroH2A.1 and macroH2A.2. The mechanisms that produce the domains of macroH2A enrichment are not known. Noncoding RNAs could be involved, since it has been shown that Xist RNA is required to maintain the enrichment of macroH2A.1 on the inactive X chromosome (40, 41).

Do macroH2A nucleosomes directly regulate gene expression? Our previous studies of macroH2A.1 distribution in adult liver showed that most of the genes that had PCR-confirmed increased expression in *macroH2A1* KO liver were enriched for macroH2A.1 (24). In contrast, most active genes that we examined showed substantial macroH2A.1 depletion. This indicates that macroH2A.1 nucleosomes have a direct repressive effect on the expression of these genes. We used our previous genome-wide analysis of the macroH2A.1 content of genes in adult mouse liver (24) to examine the macroH2A.1 content of the new genes we discovered to have altered expression in adult double KO liver. This analysis shows 2.4-fold enrichment of macroH2A.1 on *Lcn13* ($P < 0.0003$) and 2.8-fold enrichment on *Cml5* ($P < 8 \times 10^{-5}$). Therefore, we believe that these genes are excellent candidates for direct macroH2A-mediated regulation. Interestingly, *Lcn13* had a large decrease in expression in the absence of macroH2A.1 and/or

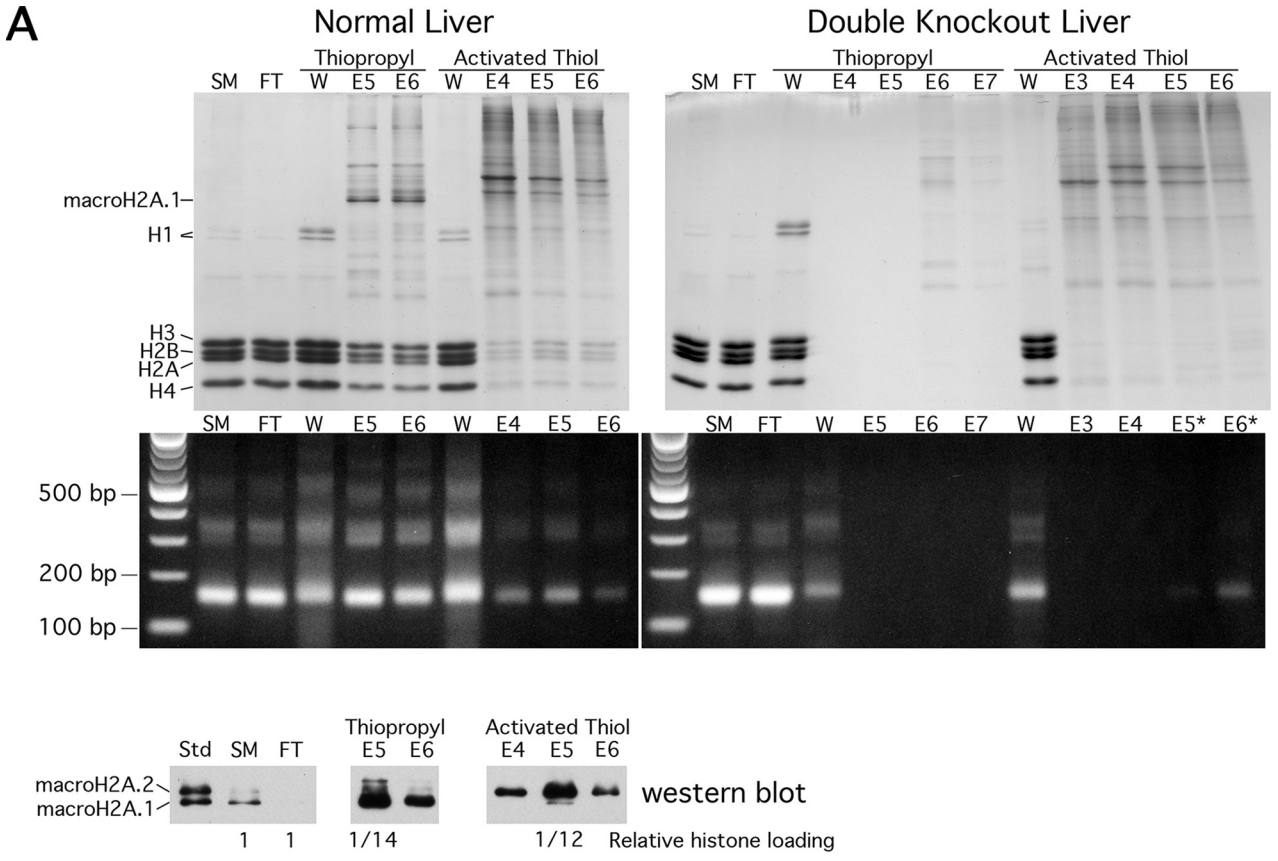
A
Normal Liver
Double Knockout Liver
Thiopropyl
Activated Thiol
SM FT W E5 E6 W E4 E5 E6
SM FT W E4 E5 E6 E7 W E3 E4 E5 E6
macroH2A.1
H1
H3
H2B
H2A
H4
SM FT W E5 E6 W E4 E5 E6
SM FT W E5 E6 E7 W E3 E4 E5* E6*
500 bp
200 bp
100 bp
Std SM FT
Thiopropyl E5 E6
Activated Thiol E4 E5 E6
macroH2A.2
macroH2A.1
western blot
1 1 1/14 1/12 Relative histone loading

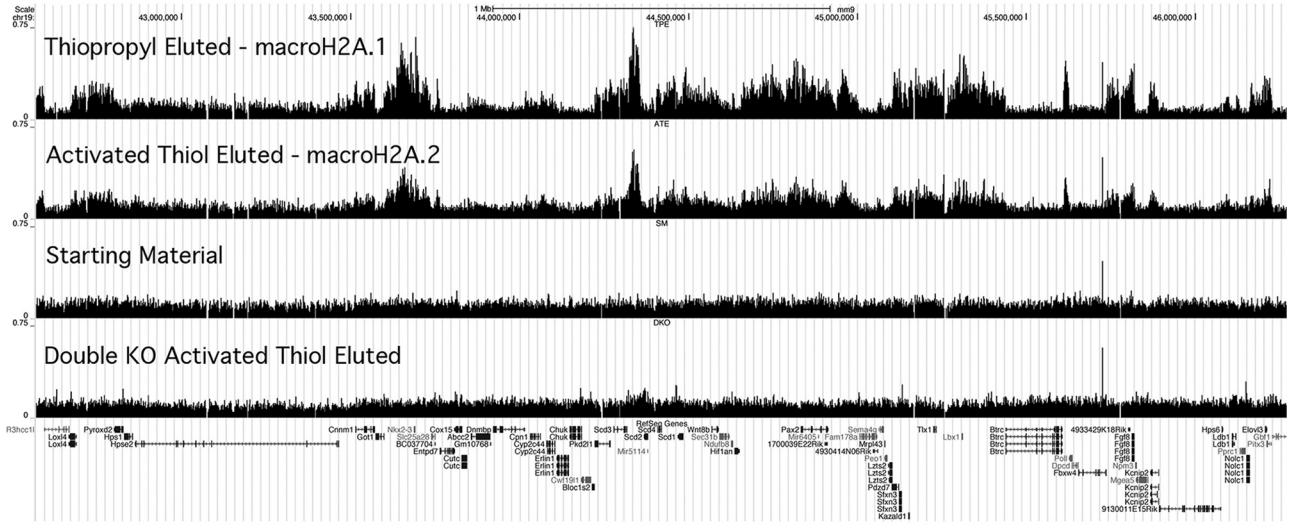
B
Thiopropyl Eluted - macroH2A.1
Activated Thiol Eluted - macroH2A.2
Starting Material
Double KO Activated Thiol Eluted
RefSeq Genes

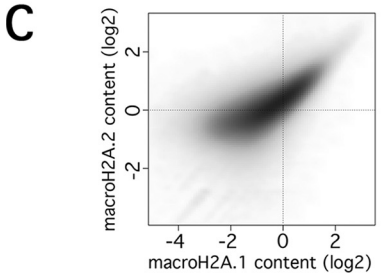
C
macroH2A.2 content (log2)
macroH2A.1 content (log2)
-4 -2 0 2
2 0 -2

macroH2A.2, indicating that macroH2A-containing nucleosomes enhance *Lcn13* expression, in contrast to the repressive effect that we have observed for most macroH2A.1 target genes. It is less clear whether macroH2As directly regulate *Pip5k1b*, *Lepr*, and *Rgs16* since these genes do not show macroH2A.1 enrichment. However, unlike most active genes, which show substantial macroH2A depletion, these genes have a neutral macroH2A.1 content, indicating that they have macroH2A nucleosomes on their transcribed regions and thus may be directly regulated by macroH2As. *Fabp5* and *Sdf2l1* are depleted of macroH2A.1 in adult liver, suggesting that they may be indirectly affected by the absence of macroH2As. However, these genes also did not show a significant change in expression in nonfasting double KO adult liver, leaving open the possibility that fasting affects the distribution of macroH2A nucleosomes on these genes. Our fetal liver macroH2A maps are not useful for *Npy*, because it is expressed from hepatic sympathetic neurons.

DISCUSSION

Our current studies show that growth and reproduction can be adversely affected by the absence of macroH2As, and we previously found reduced glucose tolerance in *macroH2A1* KO mice (23). These effects on important physiological processes can explain the evolutionary conservation of macroH2A histones. We did not see evidence that macroH2As have a crucial role in differentiation or morphogenesis during embryonic development, in contrast to some studies of *in vitro* ES cell differentiation and early zebrafish development (20–22). Interestingly, other studies of ES cells (42) or induced pluripotent stem cells (43) found that macroH2As are not required for *in vitro* differentiation and thus appear to be compatible with our results with *macroH2A* KO mice. While the increased perinatal death that we see in C57BL/6 double KOs could involve developmental defects that are not morphologically obvious, we feel that it is more likely the result of reduced vigor caused by changes in gene expression, such as those we have observed in the liver. Our genome-wide microarray analysis of double KO fetal liver showed very limited effects on gene expression, which clearly indicates that liver differentiation has not been significantly perturbed by the absence of macroH2As. It seems likely that our findings with *macroH2A* KO mice are relevant to other species, particularly closely related vertebrate species. The apparent loss of macroH2A from multiple branches of invertebrate evolution suggests that macroH2A does not have an essential developmental role in invertebrates, but the possibility that macroH2A has an essential developmental role in some species cannot be ruled out.

Our studies of *macroH2A* double KO mouse liver indicate that macroH2As function as very specific regulators of gene expression. While the expression of most genes is little affected by the absence of macroH2As, some genes show rather large effects, e.g., the 16-fold reduction in *Lcn13* expression. This gene shows significant macroH2A.1 enrichment, as do many but not all genes that have large and significant changes in expression in macroH2A KOs. This leads us to believe that many of these genes are being directly regulated by macroH2A nucleosomes, especially since most active genes show obvious macroH2A.1 depletion (24). Our results, as well as those of other studies (13), indicate that macroH2As can have positive as well as negative effects on expression. Our current results add to this complexity in showing that the same gene can be affected positively or negatively depending on nutritional status, or on which macroH2A was knocked out. The mechanisms by which macroH2As exert negative and positive effects on gene expression *in vivo* are not known.

We believe that macroH2As are being used to bring about coordinated adaptive changes in gene expression. In adult liver, those effects appear to be focused on metabolism, especially fatty acid/lipid metabolism, e.g., *Lcn13* and *Fabp5* encode lipid/fatty acid binding proteins; *Lepr* encodes the receptor for leptin, a key adipokine; and *Rgs16* encodes a GTPase-activating protein that appears to regulate fatty acid and glucose metabolism in the liver (38). The scope of macroH2A-dependent gene regulation increases in adult liver in comparison to fetal liver. There are major changes in growth and diet during the transition from newborn to young adult, and macroH2As could contribute to adapting liver functions to these changes. Our results also indicate that fasting can significantly affect macroH2A-dependent gene regulation. For example, the effects of a *macroH2A* double KO on *Fabp5*, *Rgs16*, and *Sdf2l1* were not seen in nonfasting adult liver, and the absence of macroH2A increased *Cml5* expression in fasting liver but reduced its expression in nonfasting liver. These results indicate that macroH2As could have a role in adapting liver function to changes in nutritional status.

The preferential localization of macroH2As to some domains of transcriptionally silent chromatin such as the inactive X suggests a role in maintenance of transcriptional silencing. While evidence for such a role has been detected for the inactive X chromosome (44, 45), a cell-type-specific gene (19), and the induction of pluripotency (43, 46, 47), our study of *macroH2A* double KO liver did not detect obvious derepression of genes that should be silent in the liver. Our studies of whole tissues cannot rule out the derepression of silent genes in a small percentage of cells or widespread derepression resulting in a very low level of expression. It is not surprising that we did not detect any obvious effect of *macroH2A* knockouts on X inactivation, because other studies found that loss of macroH2A leads to reactivation of the inactive X in only a small percentage of cells and that this effect requires other substantial treatments such as inhibition of DNA methylation and histone deacetylation (44, 45). Increased X reactivation could increase the occurrence of cancer (48), as could reactivation of pluripotency genes or defects in silencing associated with cellular se-

FIG 4 Overlapping distributions of macroH2A.1 and macroH2A.2 nucleosomes in fetal liver. (A) Purification of macroH2A.1 and macroH2A.2 nucleosomes from 50 fetal mouse livers by thioaffinity chromatography (see Materials and Methods). SDS gels (top panels) show the protein compositions of the fractions. Extracted DNAs were analyzed on agarose gels (below the SDS gels). Western blots of selected fractions (bottom); the relative core histone loadings on the Western blot were estimated from Coomassie blue-stained SDS gels (see Fig. S3 in the supplemental material). A control experiment that used 50 double KO fetal livers is shown on the right. Asterisks indicate that we loaded twice as much DNA in these lanes relative to the starting material to show the presence of nucleosomal DNA in these fractions. SM, starting material; FT, flowthrough fraction; W, nucleosomes washed off thiopropyl or activated thiol Sepharose columns by 0.5 M NaCl; E, thiopropyl or activated thiol fractions that were eluted with β-mercaptoethanol. (B) Mononucleosomal DNAs from the thioaffinity-purified macroH2A nucleosomes were sequenced and mapped to the mouse genome, mm9. A region of chromosome 19 is shown. The scale on the tracks is reads per million reads. (C) Plot of macroH2A.1 versus macroH2A.2 content across the genome (see Materials and Methods).

nescence. We have not observed an obvious increase in tumors in double KO mice, including small groups of double KO and wild-type mice that we kept for more than 1.5 years. Detection of such effects may require larger studies of aging mice or the use of mice predisposed to tumor formation. Thus, while macroH2As likely have a role in maintaining the silence of the inactive X and other targets, our studies of *macroH2A* double KO mice indicate that this function is masked to a large extent by other silencing mechanisms. Upregulation of other silencing mechanisms could compensate for the loss of macroH2A. One possibility is macroH2A itself, but we did not see any increase in macroH2A.2 in response to the loss of macroH2A.1, or of macroH2A.1 in response to the loss of macroH2A.2 (23) (see Fig. S2 in the supplemental material). A previous study examined the repressive chromatin modification H3K27me3, which showed significant overlap with macroH2A in dermal fibroblasts. Interestingly, the absence of macroH2As did not significantly change H3K27me3 in the regions examined (43).

We believe that macroH2A-dependent regulation of gene expression can explain the physiological effects that we observed in macroH2A knockout mice. Based on the widespread expression of macroH2As that we have seen (9, 11; also unpublished results), it seems likely that the functions of many tissues and organs are affected by macroH2As. What activities might macrodomains bring to macroH2A function? One very appealing possibility is that they function as metabolic sensors by binding specific metabolites or signaling molecules (49). This idea seems consistent with our discovery that *macroH2A* knockouts have specific effects on the expression of genes related to metabolism and metabolic regulation. ADP-ribose or related molecules may be functional ligands for macroH2A.1.1 (6, 50). However, there is not yet a clear link between this interaction and the function of macroH2A.1.1 in chromatin, and potential small-molecule regulators have not been identified for macroH2A.1.2 and macroH2A.2. Another interesting possibility based on recent findings with other macrodomain proteins (51–53) is that macroH2A macrodomains have enzymatic activities that are crucial to their function. Progress in this challenging area will be important for fully understanding the functions of these unusual core histones.

ACKNOWLEDGMENTS

This work was supported by Public Health Service grant GM49351 from the National Institute of General Medical Sciences (J.R.P.). We acknowledge support from the Penn Diabetes Endocrine Research Center grant (P30DK19525).

We thank John Tobias, Shilpa Rao, and Jonathan Schug for assistance with data analysis; Tobias Raabe and Penn Gene Targeting Core and Laboratory for assistance with the *macroH2A2* knockout; and William Beltran, Amy Durham, and Angela Brice for assistance with the eye phenotypes and histopathology analyses. We also acknowledge the services of the Mouse Phenotyping, Physiology and Metabolism Core.

REFERENCES

1. **Pehrson JR, Fried VA.** 1992. MacroH2A, a core histone containing a large nonhistone region. Science **257:**1398–1400. http://dx.doi.org/10.1126/science.1529340.
2. **Changolkar LN, Pehrson JR.** 2002. Reconstitution of nucleosomes with histone macroH2A1.2. Biochemistry **41:**179–184. http://dx.doi.org/10.1021/bi0157417.
3. **Pehrson JR, Fuji RN.** 1998. Evolutionary conservation of macroH2A subtypes and domains. Nucleic Acids Res. **26:**2837–2842. http://dx.doi.org/10.1093/nar/26.12.2837.
4. **Allen MD, Buckle AM, Cordell SC, Lowe J, Bycroft M.** 2003. The crystal structure of AF1521 a protein from Archaeoglobus fulgidus with homology to the non-histone domain of macroH2A. J. Mol Biol. **330:**503–511. http://dx.doi.org/10.1016/S0022-2836(03)00473-X.
5. **Karras GI, Kustatscher G, Buhecha HR, Allen MD, Pugieux C, Sait F, Bycroft M, Ladurner AG.** 2005. The macro domain is an ADP-ribose binding module. EMBO J. **24:**1911–1920. http://dx.doi.org/10.1038/sj.emboj.7600664.
6. **Kustatscher G, Hothorn M, Pugieux C, Scheffzek K, Ladurner AG.** 2005. Splicing regulates NAD metabolite binding to histone macroH2A. Nat. Struct. Mol. Biol. **12:**624–625. http://dx.doi.org/10.1038/nsmb956.
7. **Talbert PB, Ahmad K, Almouzni G, Ausio J, Berger F, Bhalla PL, Bonner WM, Cande WZ, Chadwick BP, Chan SW, Cross GA, Cui L, Dimitrov SI, Doenecke D, Eirin-Lopez JM, Gorovsky MA, Hake SB, Hamkalo BA, Holec S, Jacobsen SE, Kamieniarz K, Khochbin S, Ladurner AG, Landsman D, Latham JA, Loppin B, Malik HS, Marzluff WF, Pehrson JR, Postberg J, Schneider R, Singh MB, Smith MM, Thompson E, Torres-Padilla ME, Tremethick DJ, Turner BM, Waterborg JH, Wollmann H, Yelagandula R, Zhu B, Henikoff S.** 2012. A unified phylogeny-based nomenclature for histone variants. Epigenet. Chromatin **5:**7. http://dx.doi.org/10.1186/1756-8935-5-7.
8. **Rasmussen TP, Huang T, Mastrangelo MA, Loring J, Panning B, Jaenisch R.** 1999. Messenger RNAs encoding mouse histone macroH2A1 isoforms are expressed at similar levels in male and female cells and result from alternative splicing. Nucleic Acids Res. **27:**3685–3689. http://dx.doi.org/10.1093/nar/27.18.3685.
9. **Costanzi C, Pehrson JR.** 2001. MACROH2A2, a new member of the MACROH2A core histone family. J. Biol. Chem. **276:**21776–21784. http://dx.doi.org/10.1074/jbc.M010919200.
10. **Chadwick BP, Willard HF.** 2001. Histone H2A variants and the inactive X chromosome: identification of a second macroH2A variant. Hum. Mol. Genet. **10:**1101–1113. http://dx.doi.org/10.1093/hmg/10.10.1101.
11. **Pehrson JR, Costanzi C, Dharia C.** 1997. Developmental and tissue expression patterns of histone macroH2A1 subtypes. J. Cell. Biochem. **65:**107–113. http://dx.doi.org/10.1002/(SICI)1097-4644(199704)65:1<107::AID-JCB11>3.0.CO;2-H.
12. **Sporn JC, Kustatscher G, Hothorn T, Collado M, Serrano M, Muley T, Schnabel P, Ladurner AG.** 2009. Histone macroH2A isoforms predict the risk of lung cancer recurrence. Oncogene **28:**3423–3428. http://dx.doi.org/10.1038/onc.2009.26.
13. **Gamble MJ, Frizzell KM, Yang C, Krishnakumar R, Kraus WL.** 2010. The histone variant macroH2A1 marks repressed autosomal chromatin, but protects a subset of its target genes from silencing. Genes Dev. **24:**21–32. http://dx.doi.org/10.1101/gad.1876110.
14. **Costanzi C, Pehrson JR.** 1998. Histone macroH2A1 is concentrated in the inactive X chromosome of female mammals. Nature **393:**599–601. http://dx.doi.org/10.1038/31275.
15. **Costanzi C, Stein P, Worrad DM, Schultz RM, Pehrson JR.** 2000. Histone macroH2A1 is concentrated in the inactive X chromosome of female preimplantation embryos. Development **127:**2283–2289.
16. **Grigoryev SA, Nikitina T, Pehrson JR, Singh PB, Woodcock CL.** 2004. Dynamic relocation of epigenetic chromatin markers reveals an active role of constitutive heterochromatin in the transition from proliferation to quiescence. J. Cell Sci. **117:**6153–6162. http://dx.doi.org/10.1242/cs.01537.
17. **Hoyer-Fender S, Costanzi C, Pehrson JR.** 2000. Histone macroH2A1.2 is concentrated in the XY-body by the early pachytene stage of spermatogenesis. Exp. Cell Res. **258:**254–260. http://dx.doi.org/10.1006/excr.2000.4951.
18. **Zhang R, Poustovoitov MV, Ye X, Santos HA, Chen W, Daganzo SM, Erzberger JP, Serebriiskii IG, Canutescu AA, Dunbrack RL, Pehrson JR, Berger JM, Kaufman PD, Adams PD.** 2005. Formation of macroH2A-containing senescence-associated heterochromatin foci and senescence driven by ASF1a and HIRA. Dev. Cell **8:**19–30. http://dx.doi.org/10.1016/j.devcel.2004.10.019.
19. **Agelopoulos M, Thanos D.** 2006. Epigenetic determination of a cell-specific gene expression program by ATF-2 and the histone variant macroH2A. EMBO J. **25:**4843–4853. http://dx.doi.org/10.1038/sj.emboj.7601364.
20. **Buschbeck M, Uribesalgo I, Wibowo I, Rue P, Martin D, Gutierrez A, Morey L, Guigo R, Lopez-Schier H, Di Croce L.** 2009. The histone variant macroH2A is an epigenetic regulator of key developmental genes.

Nat. Struct. Mol. Biol. **16:**1074–1079. http://dx.doi.org/10.1038/nsmb.1665.

21. **Creppe C, Janich P, Cantarino N, Noguera M, Valero V, Musulen E, Douet J, Posavec M, Martin-Caballero J, Sumoy L, Di Croce L, Benitah SA, Buschbeck M.** 2012. MacroH2A1 regulates the balance between self-renewal and differentiation commitment in embryonic and adult stem cells. Mol. Cell. Biol. **32:**1442–1452. http://dx.doi.org/10.1128/MCB.06323-11.
22. **Barrero MJ, Sese B, Marti M, Izpisua Belmonte JC.** 2013. Macro histone variants are critical for the differentiation of human pluripotent cells. J. Biol Chem. **288:**16110–16116. http://dx.doi.org/10.1074/jbc.M113.466144.
23. **Changolkar LN, Costanzi C, Leu NA, Chen D, McLaughlin KJ, Pehrson JR.** 2007. Developmental changes in histone macroH2A1-mediated gene regulation. Mol. Cell. Biol. **27:**2758–2764. http://dx.doi.org/10.1128/MCB.02334-06.
24. **Changolkar LN, Singh G, Cui K, Berletch JB, Zhao K, Disteche CM, Pehrson JR.** 2010. Genome-wide distribution of macroH2A1 histone variants in mouse liver chromatin. Mol. Cell. Biol. **30:**5473–5483. http://dx.doi.org/10.1128/MCB.00518-10.
25. **Tybulewicz VL, Crawford CE, Jackson PK, Bronson RT, Mulligan RC.** 1991. Neonatal lethality and lymphopenia in mice with a homozygous disruption of the c-abl proto-oncogene. Cell **65:**1153–1163. http://dx.doi.org/10.1016/0092-8674(91)90011-M.
26. **Eggan K, Akutsu H, Loring J, Jackson-Grusby L, Klemm M, Rideout WM, III, Yanagimachi R, Jaenisch R.** 2001. Hybrid vigor, fetal overgrowth, and viability of mice derived by nuclear cloning and tetraploid embryo complementation. Proc. Natl. Acad. Sci. U. S. A. **98:**6209–6214. http://dx.doi.org/10.1073/pnas.101118898.
27. **Tusher VG, Tibshirani R, Chu G.** 2001. Significance analysis of microarrays applied to the ionizing radiation response. Proc. Natl. Acad. Sci. U. S. A. **98:**5116–5121. http://dx.doi.org/10.1073/pnas.091062498.
28. **Changolkar LN, Pehrson JR.** 2006. MacroH2A1 histone variants are depleted on active genes but concentrated on the inactive X. Mol. Cell. Biol. **26:**4410–4420. http://dx.doi.org/10.1128/MCB.02258-05.
29. **Pinkert CA.** 2002. Transgenic animal technology: a laboratory handbook, 2nd ed. Academic Press, Amsterdam, Netherlands.
30. **Nishizawa M, Shiota M, Moore MC, Gustavson SM, Neal DW, Cherrington AD.** 2008. Intraportal administration of neuropeptide Y and hepatic glucose metabolism. Am. J. Physiol. Regul. Integr. Comp. Physiol. **294:**R1197–R1204. http://dx.doi.org/10.1152/ajpregu.00903.2007.
31. **Wang Y, Chen X, Lian L, Tang T, Stalker TJ, Sasaki T, Kanaho Y, Brass LF, Choi JK, Hartwig JH, Abrams CS.** 2008. Loss of PIP5KIbeta demonstrates that PIP5KI isoform-specific PIP2 synthesis is required for IP3 formation. Proc. Natl. Acad. Sci. U. S. A. **105:**14064–14069. http://dx.doi.org/10.1073/pnas.0804139105.
32. **Wang Y, Li G, Goode J, Paz JC, Ouyang K, Screaton R, Fischer WH, Chen J, Tabas I, Montminy M.** 2012. Inositol-1,4,5-trisphosphate receptor regulates hepatic gluconeogenesis in fasting and diabetes. Nature **485:**128–132. http://dx.doi.org/10.1038/nature10988.
33. **Popsueva AE, Luchinskaya NN, Ludwig AV, Zinovjeva OY, Poteryaev DA, Feigelman MM, Ponomarev MB, Berekelya L, Belyavsky AV.** 2001. Overexpression of camello, a member of a novel protein family, reduces blastomere adhesion and inhibits gastrulation in Xenopus laevis. Dev. Biol. **234:**483–496. http://dx.doi.org/10.1006/dbio.2001.0261.
34. **Maeda K, Cao H, Kono K, Gorgun CZ, Furuhashi M, Uysal KT, Cao Q, Atsumi G, Malone H, Krishnan B, Minokoshi Y, Kahn BB, Parker RA, Hotamisligil GS.** 2005. Adipocyte/macrophage fatty acid binding proteins control integrated metabolic responses in obesity and diabetes. Cell Metab. **1:**107–119. http://dx.doi.org/10.1016/j.cmet.2004.12.008.
35. **Cho KW, Zhou Y, Sheng L, Rui L.** 2011. Lipocalin-13 regulates glucose metabolism by both insulin-dependent and insulin-independent mechanisms. Mol. Cell. Biol. **31:**450–457. http://dx.doi.org/10.1128/MCB.00459-10.
36. **Sheng L, Cho KW, Zhou Y, Shen H, Rui L.** 2011. Lipocalin 13 protein protects against hepatic steatosis by both inhibiting lipogenesis and stimulating fatty acid beta-oxidation. J. Biol. Chem. **286:**38128–38135. http://dx.doi.org/10.1074/jbc.M111.256677.
37. **Brennan AM, Mantzoros CS.** 2006. Drug insight: the role of leptin in human physiology and pathophysiology—emerging clinical applications. Nat. Clin. Pract. Endocrinol. Metab. **2:**318–327. http://dx.doi.org/10.1038/ncpendmet0196.
38. **Pashkov V, Huang J, Parameswara VK, Kedzierski W, Kurrasch DM, Tall GG, Esser V, Gerard RD, Uyeda K, Towle HC, Wilkie TM.** 2011. Regulator of G protein signaling (RGS16) inhibits hepatic fatty acid oxidation in a carbohydrate response element-binding protein (ChREBP)-dependent manner. J. Biol. Chem. **286:**15116–15125. http://dx.doi.org/10.1074/jbc.M110.216234.
39. **Chakravarthy S, Luger K.** 2006. The histone variant macro-H2A preferentially forms "hybrid nucleosomes." J. Biol. Chem. **281:**25522–25531. http://dx.doi.org/10.1074/jbc.M602258200.
40. **Csankovszki G, Panning B, Bates B, Pehrson JR, Jaenisch R.** 1999. Conditional deletion of Xist disrupts histone macroH2A localization but not maintenance of X inactivation. Nat. Genet. **22:**323–324. http://dx.doi.org/10.1038/11887.
41. **Beletskii A, Hong Y-K, Pehrson J, Egholm M, Strauss WM.** 2001. PNA interference mapping demonstrates functional domains in the noncoding RNA Xist. Proc. Natl. Acad. Sci. U. S. A. **98:**9215–9220. http://dx.doi.org/10.1073/pnas.161173098.
42. **Tanasijevic B, Rasmussen TP.** 2011. X chromosome inactivation and differentiation occur readily in ES cells doubly-deficient for macroH2A1 and macroH2A2. PLoS One **6:**e21512. http://dx.doi.org/10.1371/journal.pone.0021512.
43. **Gaspar-Maia A, Qadeer ZA, Hasson D, Ratnakumar K, Leu NA, Leroy G, Liu S, Costanzi C, Valle-Garcia D, Schaniel C, Lemischka I, Garcia B, Pehrson JR, Bernstein E.** 2013. MacroH2A histone variants act as a barrier upon reprogramming towards pluripotency. Nat. Commun. **4:**1565. http://dx.doi.org/10.1038/ncomms2582.
44. **Hernandez-Munoz I, Lund AH, van der Stoop P, Boutsma E, Muijrers I, Verhoeven E, Nusinow DA, Panning B, Marahrens Y, van Lohuizen M.** 2005. Stable X chromosome inactivation involves the PRC1 Polycomb complex and requires histone MACROH2A1 and the CULLIN3/SPOP ubiquitin E3 ligase. Proc. Natl. Acad. Sci. U. S. A. **102:**7635–7640. http://dx.doi.org/10.1073/pnas.0408918102.
45. **Pasque V, Gillich A, Garrett N, Gurdon JB.** 2011. Histone variant macroH2A confers resistance to nuclear reprogramming. EMBO J. **30:**2373–2387. http://dx.doi.org/10.1038/emboj.2011.144.
46. **Pasque V, Radzisheuskaya A, Gillich A, Halley-Stott RP, Panamarova M, Zernicka-Goetz M, Surani MA, Silva JC.** 2012. Histone variant macroH2A marks embryonic differentiation in vivo and acts as an epigenetic barrier to induced pluripotency. J. Cell Sci. **125:**6094–6104. http://dx.doi.org/10.1242/jcs.113019.
47. **Barrero MJ, Sese B, Kuebler B, Bilic J, Boue S, Marti M, Izpisua Belmonte JC.** 2013. Macrohistone variants preserve cell identity by preventing the gain of H3K4me2 during reprogramming to pluripotency. Cell Rep. **3:**1005–1011. http://dx.doi.org/10.1016/j.celrep.2013.02.029.
48. **Yildirim E, Kirby JE, Brown DE, Mercier FE, Sadreyev RI, Scadden DT, Lee JT.** 2013. Xist RNA is a potent suppressor of hematologic cancer in mice. Cell **152:**727–742. http://dx.doi.org/10.1016/j.cell.2013.01.034.
49. **Ladurner AG.** 2006. Rheostat control of gene expression by metabolites. Mol. Cell **24:**1–11. http://dx.doi.org/10.1016/j.molcel.2006.09.002.
50. **Timinszky G, Till S, Hassa PO, Hothorn M, Kustatscher G, Nijmeijer B, Colombelli J, Altmeyer M, Stelzer EH, Scheffzek K, Hottiger MO, Ladurner AG.** 2009. A macrodomain-containing histone rearranges chromatin upon sensing PARP1 activation. Nat. Struct. Mol. Biol. **16:**923–929. http://dx.doi.org/10.1038/nsmb.1664.
51. **Slade D, Dunstan MS, Barkauskaite E, Weston R, Lafite P, Dixon N, Ahel M, Leys D, Ahel I.** 2011. The structure and catalytic mechanism of a poly(ADP-ribose) glycohydrolase. Nature **477:**616–620. http://dx.doi.org/10.1038/nature10404.
52. **Sharifi R, Morra R, Appel CD, Tallis M, Chioza B, Jankevicius G, Simpson MA, Matic I, Ozkan E, Golia B, Schellenberg MJ, Weston R, Williams JG, Rossi MN, Galehdari H, Krahn J, Wan A, Trembath RC, Crosby AH, Ahel D, Hay R, Ladurner AG, Timinszky G, Williams RS, Ahel I.** 2013. Deficiency of terminal ADP-ribose protein glycohydrolase TARG1/C6orf130 in neurodegenerative disease. EMBO J. **32:**1225–1237. http://dx.doi.org/10.1038/emboj.2013.51.
53. **Rosenthal F, Feijs KL, Frugier E, Bonalli M, Forst AH, Imhof R, Winkler HC, Fischer D, Caflisch A, Hassa PO, Luscher B, Hottiger MO.** 2013. Macrodomain-containing proteins are new mono-ADP-ribosylhydrolases. Nat. Struct. Mol. Biol. **20:**502–507. http://dx.doi.org/10.1038/nsmb.2521.